JOURNAL OF INDUSTRIAL AND
MANAGEMENT OPTIMIZATION
Volume **11**, Number **4**, October **2015**

doi:10.3934/jimo.2015.11.xx

pp. **X–XX**

MODELLING AND OPTIMAL CONTROL OF BLOOD GLUCOSE LEVELS IN THE HUMAN BODY

Zahra Al Helal, Volker Rehbock and Ryan Loxton

Department of Mathematics and Statistics, Curtin University
GPO Box U1987 Perth, Western Australia 6845, Australia

(Communicated by Jie Sun)

Abstract. Regulating the blood glucose level is a challenging control problem for the human body. Abnormal blood glucose levels can cause serious health problems over time, including diabetes. Although several mathematical models have been proposed to describe the dynamics of glucose-insulin interaction, none of them have been universally adopted by the research community. In this paper, we consider a dynamic model of the blood glucose regulatory system originally proposed by Liu and Tang in 2008. This model consists of eight state variables naturally divided into three subsystems: the glucagon and insulin transition subsystem, the receptor binding subsystem and the glucose subsystem. The model contains 36 model parameters, many of which are unknown and difficult to determine accurately. We formulate an optimal parameter selection problem in which optimal values for the model parameters must be selected so that the resulting model best fits given experimental data. We demonstrate that this optimal parameter selection problem can be solved readily using the optimal control software MISER 3.3. Using this approach, significant improvements can be made in matching the model to the experimental data. We also investigate the sensitivity of the resulting optimized model with respect to the insulin release rate. Finally, we use MISER 3.3 to determine optimal open loop controls for the optimized model.

1. **Introduction.** Blood glucose is crucial to maintaining health. The normal concentration of blood glucose in a healthy person is between 80 to 120 (mg/dl); concentrations beyond this range may cause hyperglycaemia (above 120) or hypoglycaemia (under 80). Prolonged irregularities in the blood glucose level can result in major health problems such as diabetes, an incurable disease caused when the pancreas no longer makes insulin (type 1 diabetes), or when the pancreas cannot make enough insulin and the body develops insulin resistance (type 2 diabetes). Diabetes is considered a major international health problem. Approximately 3.61 million Australians have diabetes or pre-diabetes, and 366 million people have diabetes worldwide [3].

To date, several mathematical models for the blood glucose regulatory system have been proposed. These models aim to describe the glucose-insulin interaction within the human body. The Bergman minimal model (1980) is considered to be the fundamental model in this area [1]. Several control models, such as proportional-integral-derivative (PID) control [10], robust servo control [6], and model predictive

2010 *Mathematics Subject Classification.* Primary: 49M37; Secondary: 65P99, 92C45, 92C50.
Key words and phrases. Blood glucose, optimal control, dynamic model, optimal parameter selection problem.

control (MPC) [2], have been developed based on the Bergman minimal model. In most of the existing models, the glucose regulatory system is greatly simplified and only glucose and insulin are considered.

Liu and Tang [8] have developed a new feedback control model at the molecular level, which considers the role of the liver, the glucagon and insulin signaling pathways and the conversion between glucose and glycogen. However, one of the difficulties in working with this model is that it contains many model parameters that are not well-defined. Thus, in this paper, we formulate an optimal parameter selection problem that can be solved using the software package MISER 3.3 [4]. As we will see, this approach results in significant improvements in matching the model to experimental data.

This paper is organized as follows. We first introduce the dynamic model of blood glucose levels proposed in [8] in Section 2. Then, in Section 3, we formulate an optimal parameter selection problem to determine optimal values for the uncertain model parameters in the dynamic model. The objective here is to match the model to given experimental data as closely as possible. For this purpose, we consider three possible objective functions and solve the resulting problems using MISER 3.3. In Section 4, we perform a sensitivity test, as proposed in Liu and Tang [8], on the resulting optimized model to test its sensitivity with respect to the insulin release rate. In Section 5, based on the optimized model, we formulate an optimal control problem in which the aim is to optimize the release rate for both insulin and glucose. This optimal control problem can also be solved using MISER 3.3. Finally, we conclude the paper with a discussion of the numerical results and future work.

2. **Mathematical model.**

The dynamic model in Liu and Tang [8] consists of eight state variables. These state variables are defined as follows:

x_1 = concentration of plasma glucagon (in moles per liter);
x_2 = concentration of plasma insulin (in moles per liter);
x_3 = intracellular concentration of glucagon (in moles per liter);
x_4 = intracellular concentration of insulin (in moles per liter);
x_5 = concentration of glucagon receptor (in moles per liter);
x_6 = concentration of insulin-bound receptor (in moles per liter);
x_7 = blood concentration of glycogen (in milligrams per liter);
x_8 = blood concentration of glucose (in milligrams per liter).

The model can be naturally divided into three subsystems, each of which is described below. See Figure 1 for a graphical representation.

2.1. **Insulin and glucagon transition subsystem.**

This subsystem governs x_1 and x_2. The model assumes that plasma insulin does not act directly on the glucose metabolism, but instead through remote cellular insulin. The model also assumes that intracellular insulin does not move back to plasma. Under these assumptions, the dynamics for x_1 are given by

$$\frac{dx_1}{dt} = -(k^p_{1,1} + k^p_{1,2})x_1 + w_1, \tag{1}$$

where $k^p_{1,1}$ is a transition rate, $k^p_{1,2}$ is a degradation rate, and w_1 is the glucagon release rate (GRR) defined by

$$w_1 = \frac{G_m}{1 + b_1 \exp a_1(x_8 - C_5)}. \tag{2}$$

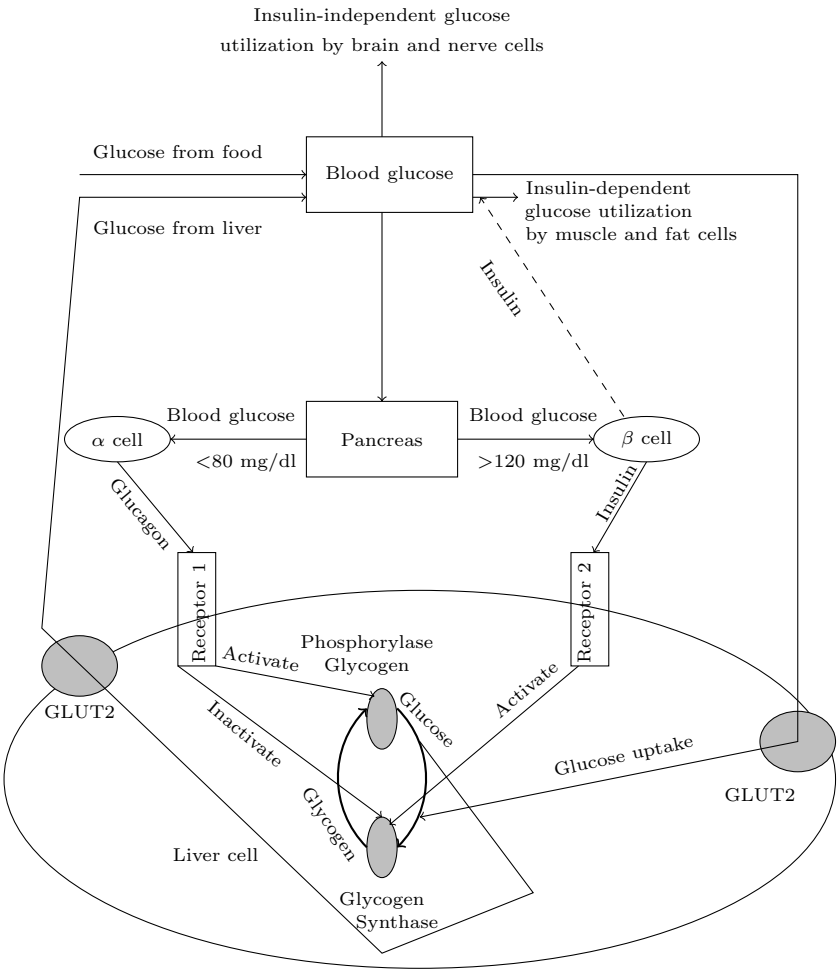

FIGURE 1. A simplified model of the regulatory system for blood glucose (adapted from reference [8]). Glucose is input from food and the liver, and used by brain and nerve cells (insulin-independent, solid arrow) and by tissue cells (insulin-dependent, dashed arrow). Glucose is transported to and from liver cells by the concentration-driven GLUT2, which is insulin-independent. In response to low blood glucose levels, the α cells of the pancreas produce the hormone glucagon. The glucagon initiates a series of activations of kinases (the black arrows indicate such activations), and which ultimately leads to the activation of the enzyme glycogen phosphorylase, to catalyze the breakdown of glycogen into glucose. In response to high blood glucose levels, the β cells of the pancreas secrete insulin. Insulin triggers reactions to activate glycogen synthase, which catalyses the conversion of glucose into glycogen.

Furthermore, the dynamics for x_2 are given by

$$\frac{dx_2}{dt} = -(k^p_{2,1} + k^p_{2,2})x_2 + w_2, \tag{3}$$

where $k^p_{2,1}$ is a transition rate, $k^p_{2,2}$ is a degradation rate, and w_2 is the insulin release rate (IRR) defined by

$$w_2 = \frac{R_m}{1 + b_2 \exp a_2(C_1 - x_8)}. \tag{4}$$

The fractions w_1 and w_2 in equations (1)-(4) model the natural feedback control mechanisms in the body. Note that G_m is the maximum glucagon infusion rate, R_m is the maximum insulin infusion rate, and a_1, a_2, b_1, b_2, C_1 and C_5 are positive constants.

2.2. **Insulin and glucagon receptor binding subsystem.** This subsystem governs x_3, x_4, x_5 and x_6. The model assumes that receptor recycling is a closed subsystem; the synthesis rate of receptors is equal to their degradation rate. The dynamics for this subsystem are given by

$$\frac{dx_3}{dt} = -k^s_{1,1}x_3(R^0_1 - x_5) - k^s_{1,2}x_3 + \frac{k^p_{1,1}V_p x_1}{V}, \tag{5}$$

$$\frac{dx_4}{dt} = -k^s_{2,1}x_4(R^0_2 - x_6) - k^s_{2,2}x_4 + \frac{k^p_{2,1}V_p x_2}{V}, \tag{6}$$

$$\frac{dx_5}{dt} = -k^s_{1,1}x_3(R^0_1 - x_5) - k^r_1 x_5, \tag{7}$$

$$\frac{dx_6}{dt} = -k^s_{2,1}x_4(R^0_2 - x_6) - k^r_2 x_6, \tag{8}$$

where $k^s_{1,1}$ and $k^s_{2,1}$ are the hormone-receptor association rates, $k^s_{1,2}$ and $k^s_{2,2}$ are the degradation rates, R^0_1 and R^0_2 are the total concentrations of receptors, k^r_1 and k^r_2 are the inactivation rates, V_p is the plasma insulin volume, and V is the cellular insulin volume.

2.3. **Glucose production and utilization subsystem.** This subsystem, which governs x_7 and x_8, models the production of glucose. Plasma glucose has two sources: hepatic glucose produced by converting glycogen into glucose in the liver and exogenous glucose taken from food. Glucose utilization can be classified into two classes: insulin-independent (by brain and nerve cells) and insulin-dependent (by the muscle and fat cells). The dynamics for x_7 are given by

$$\frac{dx_7}{dt} = f_4 - f_5, \tag{9}$$

where

$$f_4 = \frac{k_1 x_6}{1 + k_2 x_5} \cdot \frac{V^{gs}_{\max} x_8}{k^{gs}_m + x_8}, \tag{10}$$

$$f_5 = k_3 x_5 \frac{V^{gp}_{\max} x_7}{k^{gp}_m + x_7}. \tag{11}$$

Here, k_1, k_2 and k_3 are the feedback control gains, $V^{gp}_{\max}$ is the maximum velocity of glycogen phosphorylase, $V^{gs}_{\max}$ is the maximum velocity of glycogen synthase, and k^{gs}_m and k^{gp}_m are the Michaelis-Menton constants.

The dynamics for x_8 are given by

$$\frac{dx_8}{dt} = -f_4 + f_5 - f_1 - f_2 f_3 + G, \tag{12}$$

where

$$f_1 = U_b \left(1 - \exp\left(-\frac{x_8}{C_2}\right)\right), \tag{13}$$

$$f_2 = \frac{x_8}{C_3}, \tag{14}$$

$$f_3 = U_0 + \frac{(U_m - U_0)x_4^\beta}{C_4^\beta + x_4^\beta}. \tag{15}$$

Note that U_0, U_b, U_m, C_2, C_3, C_4 and β are positive constants, and G is the exogenous glucose intake derived from digesting food.

2.4. **Initial conditions and model constants.** We assume that the system is modelled over a 9 hour period, i.e., $t \in [0, 540]$, where t is the time in minutes. The initial conditions prescribed for the model in Liu and Tang [8] are

$$x_1(0) = 1.4 \times 10^{-11}, \tag{16}$$

$$x_2(0) = 1.389 \times 10^{-11}, \tag{17}$$

$$x_3(0) = 0, \tag{18}$$

$$x_4(0) = 6.945 \times 10^{-14}, \tag{19}$$

$$x_5(0) = 0, \tag{20}$$

$$x_6(0) = 0, \tag{21}$$

$$x_7(0) = 200, \tag{22}$$

$$x_8(0) = 918. \tag{23}$$

The complete model defined by equations (1)-(23) includes 36 model constants as listed in Table 1. Although Liu and Tang [8] give explicit values for each of these constants, they also acknowledge that many of these values are merely informed guesses, usually based on biological understanding or adopted from other publications. In Table 1, we have indicated which of the constants are well-defined and which have some uncertainty as to their true values. Note that the values of some of the constants in Table 1 differ from the original values given by Liu and Tang in [8]. These changes were made based on the advice received in private communication with Liu and Tang. In particular, we have changed the units of measurement for the parameters $k^s_{2,1}$, R^0_2, C_4, R_m and k_1, and we also use different values for k_i, $i = 1, 2, 3$. These new values are reported in Table 1 and used throughout this paper. In addition, Liu and Tang gave the following guidance on the behaviour of some of the uncertain parameters: the degradation rates of glucagon and its receptor ($k^s_{1,2}$, k^r_1) can be assumed to be the same as the respective rates for insulin ($k^s_{2,2}$, k^r_2); the maximum glucagon infusion rate G_m can be selected to be much smaller than R_m; a_1 and b_1 can be selected so that the glucagon secretion w_1 increases rapidly when the blood glucose level x_8 drops to around 800 mg/l; $k^p_{2,1}$ can be assumed to be the same as $k^p_{1,1}$.

3. **Parameter estimation.** Our goal in this paper is to optimize the model parameters in (1)-(23), so that the model matches experimental data as closely as possible. As in Liu and Tang [8], we use the experimental data reported in Korach-André et al. [5]. This data set consists of blood glucose measurements from a healthy individual taken after meals. We denote this data set by $\{(\tau_i, \hat{x}^i_8)\}^9_{i=1}$, where τ_i denotes the i-th observation time and $\hat{x}^i_8$ denotes the blood glucose concentration observed

Constant	Value	Unit	Status
$k^p_{1,1}$	0.14	min^{-1}	uncertain
$k^p_{2,1}$	0.14	min^{-1}	uncertain
$k^p_{1,2}$	0.3	min^{-1}	well-defined
$k^p_{2,2}$	1/6	min^{-1}	uncertain
$k^s_{1,1}$	6×10^7	$\text{M}^{-1}\ \text{min}^{-1}$	well-defined
$k^s_{2,1}$	6×10^7	$\text{M}^{-1}\ \text{min}^{-1}$	well-defined
$k^s_{1,2}$	0.01	min^{-1}	uncertain
$k^s_{2,2}$	0.01	min^{-1}	uncertain
k^r_1	0.2	min^{-1}	uncertain
k^r_2	0.2	min^{-1}	well-defined
R^0_1	9×10^{-13}	M	well-defined
R^0_2	3.6114×10^{-12}	M	well-defined
$v^{gp}_{\max}$	80	mg/l/min	uncertain
k^{gp}_m	600	mg/l	well-defined
$v^{gs}_{\max}$	3.87×10^{-4}	mg/l/min	uncertain
k^{gs}_m	67	mg/l	well-defined
k_1	$2.76900924 \times 10^{11}$	M^{-1}	well-defined
k_2	1.1111111×10^{14}	M^{-1}	well-defined
k_3	1.1111111×10^{12}	M^{-1}	well-defined
V	11	l	uncertain
V_p	3	l	uncertain
U_b	7.2	mg/l/min	uncertain
U_0	4	mg/l/min	uncertain
U_m	94	mg/l/min	uncertain
G_m	2.23×10^{-10}	M/min	uncertain
R_m	4.8615×10^{-10}	M/min	uncertain
C_1	2000	mg/l	uncertain
C_2	144	mg/l	uncertain
C_3	1000	mg/l	uncertain
C_4	5.556×10^{-10}	M/l	uncertain
C_5	1000	mg/l	uncertain
β	1.77	-	uncertain
a_1	0.005	$(\text{mg/l})^{-1}$	uncertain
a_2	1/300	$(\text{mg/l})^{-1}$	uncertain
b_1	10	-	uncertain
b_2	1	-	uncertain

TABLE 1. Constants in the dynamic model (1)-(23), where M denotes moles.

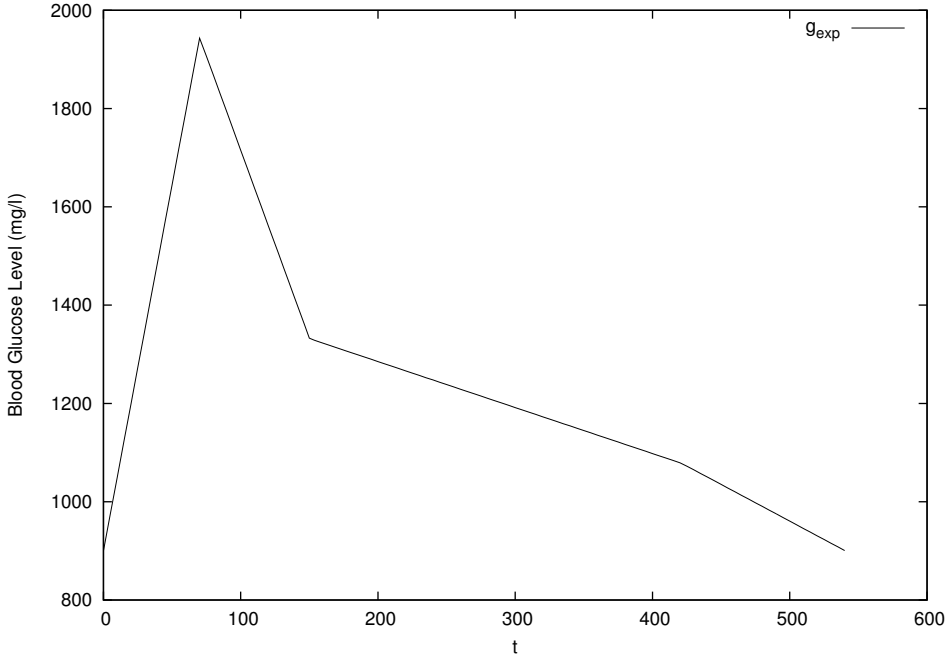

FIGURE 2. Experimental data from Korach-André et al. [5]

i	1	2	3	4	5	6	7	8	9
τ_i	0	60	120	150	180	240	380	420	540
$\hat{x}_8^i$	900	1785.29	1530.27	1330.88	1300.55	1244.95	1113.53	1078.2	900.72

TABLE 2. Experimental data from Korach-André et al. [5]

at the i-th observation time. The experimental data is shown in Figure 2 and listed in Table 2. We assume that the experimental data can be interpolated linearly as shown in Figure 2 to yield the function $g_{exp}(t)$. Using the original parameter values in Liu and Tang [8], the resulting trajectory for the blood glucose history is shown in Figure 3. We will improve the Liu-Tang model by formulating an optimal parameter selection problem to find more appropriate values for the uncertain model parameters in Table 1. To do this, for each uncertain parameter, we need to specify upper and lower bounds. For parameters V, U_b, U_0 and β, appropriate bounds were suggested by Liu and Tang [8] in our personal correspondence as shown in Table 3. For the other parameters, we use an iterative approach as follows. We initially guessed the lower and upper bounds and solved the resulting parameter estimation problem. Then, for those parameters whose optimal value was equal to the lower or upper bound, we decreased/increased the respective bound by 10 percent. This process continued until all optimal parameter values were contained in the interior of the respective intervals. This iterative approach is needed because the model (1)-(23) is quite sensitive to some of the model parameters, and is difficult to integrate numerically when the model parameter values are too far from those in the previous stage. For the purpose of model matching, we consider three possible objectives and solve the resulting parameter estimation problem with MISER 3.3.

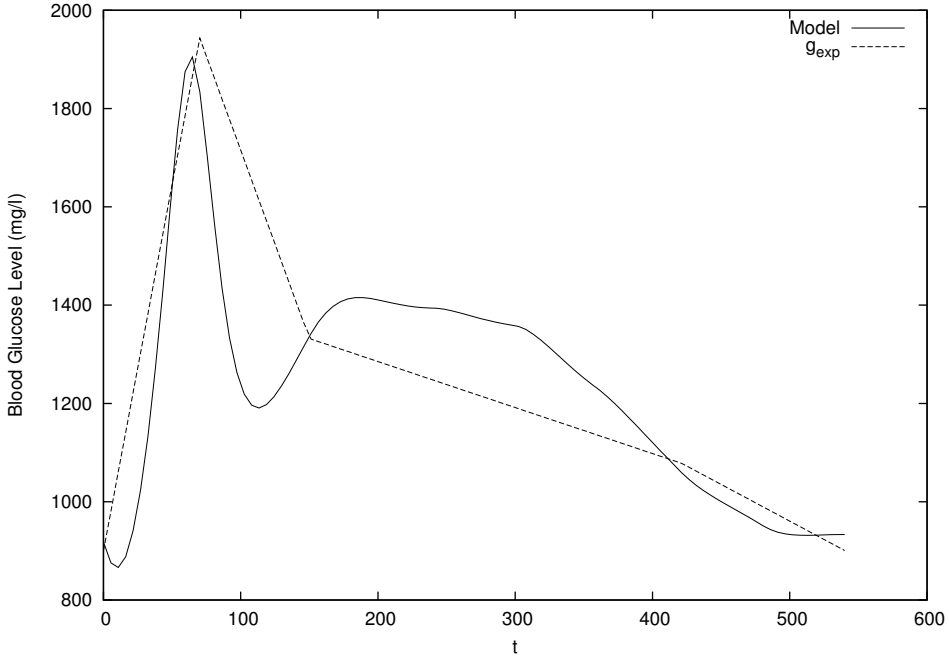

FIGURE 3. Comparison of two blood glucose trajectories: the solid trajectory is the simulated trajectory from (1)-(23) using the parameter values in Liu and Tang [8]; the dashed trajectory is the experimental data from Korach-André et al. [5]

Parameter	Lower bound	Upper bound
V	10	25
U_b	4	12
U_0	4	12
β	1	2

TABLE 3. Lower and upper bounds for V, U_b, U_0, and β

3.1. **Case 1.** In this case, our aim is to match the simulated blood glucose level to the experimental data $g_{exp}(t)$ over the entire time horizon. Thus, the aim is to minimize

$$J = \int_0^{540} (x_8(t) - g_{exp}(t))^2 \, dt \tag{24}$$

subject to the dynamic model defined by equations (1)-(23).

The glucose trajectory generated from (1)-(23) using the optimal parameter estimates is shown in Figure 4. Looking at Figures 3 and 4, it is clear that the optimal parameter estimates yield significant improvements in model accuracy compared with the estimates in [8]. However, there appears to be some mismatch between the model trajectory and experimental data at the terminal time. Hence, we consider a modified version of the objective function (24) in the next case.

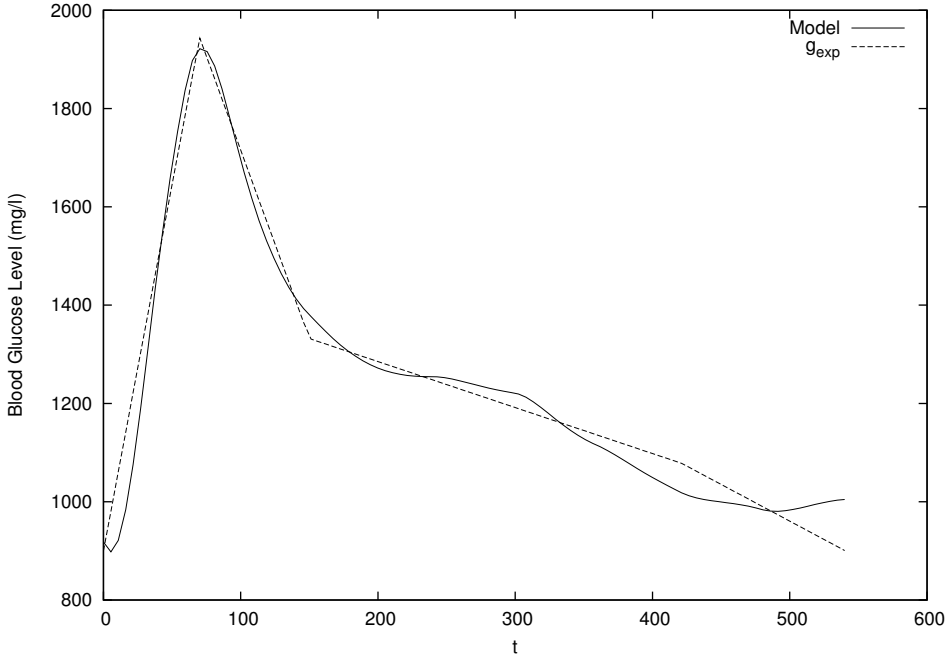

FIGURE 4. Comparison of two blood glucose trajectories: the solid trajectory is the simulated trajectory from (1)-(23) using the optimal parameter values for Case 1; the dashed trajectory is the experimental data from Korach-André et al. [5]

3.2. **Case 2.** Here, we add another term to the objective function that measures the difference between the predicted and actual blood glucose levels at the terminal time. Specifically, the aim is to minimize

$$J = w\left(x_8(540) - 900.72\right)^2 + \int_0^{540} \left(x_8(t) - g_{exp}(t)\right)^2 dt \tag{25}$$

subject to the dynamics (1)-(23), where the weight w is chosen as $w = 1000$. The idea here is to force better agreement between the model output and the experimental data at the end of the time horizon. As seen from Figure 5, this can be achieved at the expense of increased error earlier in the time horizon.

3.3. **Case 3.** Since the experimental data in Table 2 is only measured at a small number of isolated times, the actual glucose level between these times is unknown. Thus, our definition of $g_{exp}(t)$, as a piecewise linear interpolating function, and the use of the integral terms in (24) and (25), may not be appropriate. An alternative parameter estimation problem is to minimize

$$J = \sum_{i=1}^{9} \left(x_8(\tau_i) - \hat{x}_8^i\right)^2$$

subject to the dynamics (1)-(23), where $\hat{x}_8^i$ and τ_i, $i = 1, \ldots 9$, are as defined in Table 2. Note that this objective function is not in the standard canonical form due to the presence of multiple non-integral terms that depend on the state at

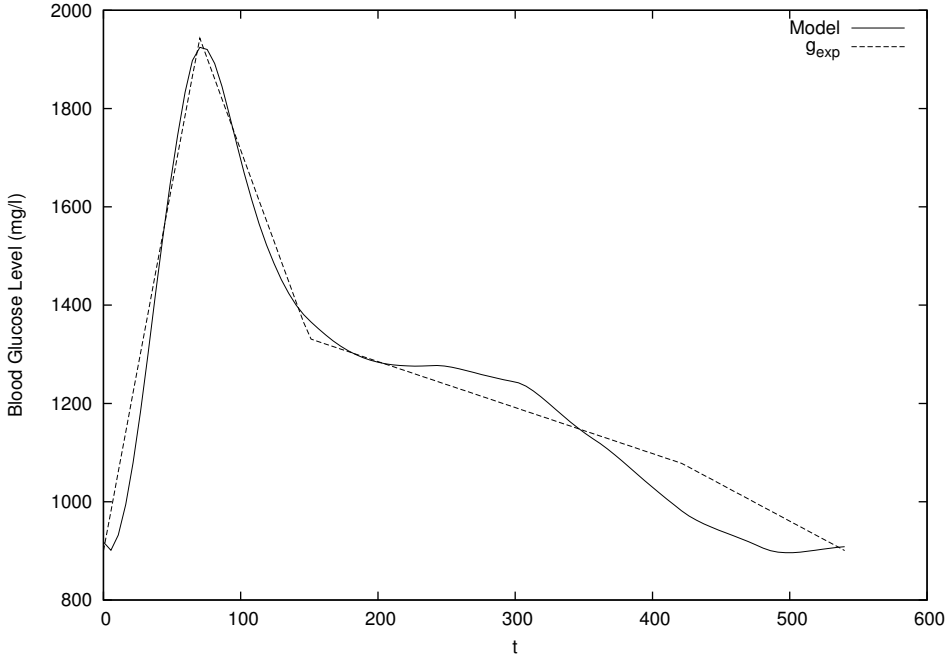

FIGURE 5. Comparison of two blood glucose trajectories: the solid trajectory is the simulated trajectory from (1)-(23) using the optimal parameter values for Case 2; the dashed trajectory is the experimental data from Korach-André et al. [5]

intermediate times (called characteristic times in the optimal control literature). Nevertheless, objective functions of this form can be handled using the techniques developed in [9] and [11], which have been incorporated into the MISER 3.3 software [4].

As shown in Figure 6, the resulting blood glucose level tracks the individual experimental measurements very closely, although as expected it does not follow the interpolating function $g_{exp}(t)$ as closely as we observed for Case 1.

4. **Model sensitivity.** The optimal parameter values for Cases 1, 2 and 3 are reported in Table 4. In Liu and Tang [8], a sensitivity test was performed by doubling and halving the insulin feedback rate and observing the corresponding model response. For comparison, we perform the same sensitivity test on the model with the optimized parameters from Case 1. This involves replacing the original insulin feedback rate w_2 in (4) by

$$w_2 = \frac{2R_m}{1 + b_2 \exp a_2(C_1 - x_8)}, \tag{26}$$

and

$$w_2 = \frac{\frac{1}{2}R_m}{1 + b_2 \exp a_2(C_1 - x_8)}, \tag{27}$$

respectively. The resulting blood glucose levels are shown in Figures 7 and 8, respectively. Compared to the corresponding figures in Liu and Tang [8], the glucose

Parameter	Original value	Case 1	Case 2	Case 3
$k^p_{1,1}$	0.14	1.28929	2.19177	1.37664
$k^p_{2,1}$	0.14	0.100804	0.114719	0.154412
$k^p_{1,2}$	0.3	0.3	0.3	0.3
$k^p_{2,2}$	1/6	0.437605	0.743780	0.743944
$k^s_{1,1}$	6×10^7	6×10^7	6×10^7	6×10^7
$k^s_{2,1}$	6×10^7	6×10^7	6×10^7	6×10^7
$k^s_{1,2}$	0.01	7.19985×10^{-3}	2.16×10^{-3}	7.6107×10^{-2}
$k^s_{2,2}$	0.01	9.52782×10^{-3}	8.5×10^{-3}	8.95549×10^{-3}
k^r_1	0.2	2.59194×10^{-2}	7.776×10^{-3}	2.4×10^{-1}
k^r_2	0.2	0.2	0.2	0.2
R^0_1	9×10^{-13}	9×10^{-13}	9×10^{-13}	9×10^{-13}
R^0_2	3.6114×10^{-12}	3.6114×10^{-12}	3.6114×10^{-12}	3.6114×10^{-12}
$v^{gp}_{\max}$	80	25.0197	24.6129	24.7160
k^{gp}_m	600	600	600	600
$v^{gs}_{\max}$	3.87×10^{-4}	3.41805×10^{-3}	5.811×10^{-3}	5.811×10^{-3}
k^{gs}_m	67	67	67	67
k_1	2.76901×10^{11}	2.76901×10^{11}	2.76901×10^{11}	2.76901×10^{11}
k_2	1.11111×10^{14}	1.11111×10^{14}	1.11111×10^{14}	1.11111×10^{14}
k_3	1.11111×10^{12}	1.11111×10^{12}	1.11111×10^{12}	1.11111×10^{12}
V	11	10.0004	10.3573	10.0181
V_p	3	2.41375	3.44929	2.77484
U_b	7.2	4	4	7.80699
U_0	4	4	4	8.14836
U_m	94	227.508	227.972	227.642
G_m	2.23×10^{-10}	2.05367×10^{-9}	3.49116×10^{-9}	1.87341×10^{-9}
R_m	4.8615×10^{-10}	2.29663×10^{-10}	3.98353×10^{-10}	4.22818×10^{-10}
C_1	2000	1114.19	1114.07	1114.29
C_2	144	345.384	345.434	345.378
C_3	1000	1061.82	1061.77	1061.77
C_4	5.556×10^{-10}	1.9556×10^{-9}	3.32383×10^{-9}	3.28142×10^{-9}
C_5	1000	1124.67	1124.67	1124.68
β	1.77	1.14055	1.17821	1.33999
a_1	0.005	3.48467×10^{-2}	5.9238×10^{-2}	5.9238×10^{-2}
a_2	1/300	1.45946×10^{-2}	8.59508×10^{-3}	8.70603×10^{-3}
b_1	10	11.4710	11.4664	11.4667
b_2	1	1.15002	1.1893	1.955

TABLE 4. Comparing the optimized parameter values with the values in [8]

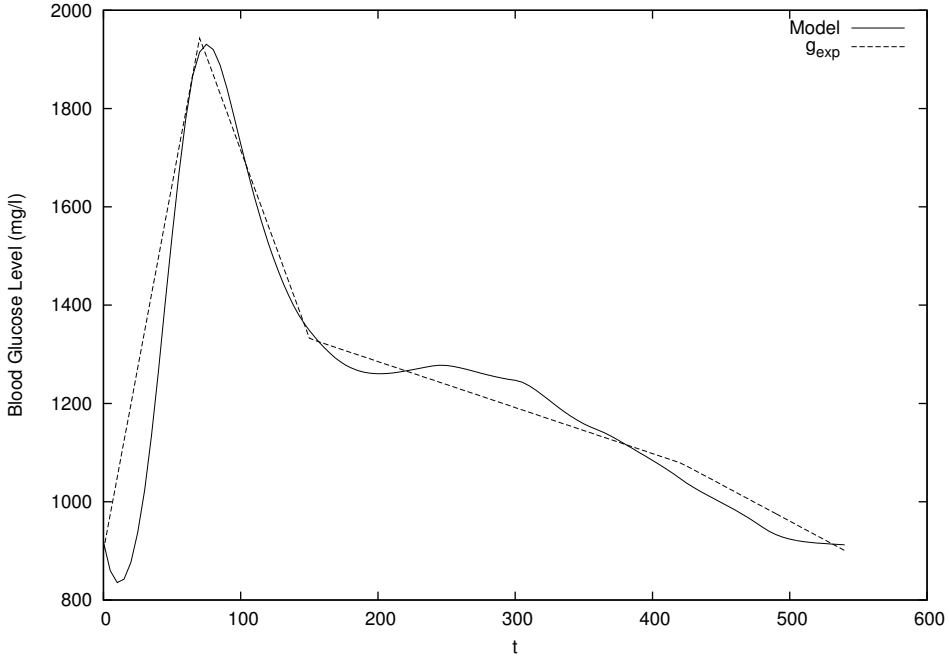

FIGURE 6. Comparison of two blood glucose trajectories: the solid trajectory is the simulated trajectory from (1)-(23) using the optimal parameter values for Case 3; the dashed trajectory is the experimental data from Korach-André et al. [5]

levels in Figures 7 and 8 are further away from the experimental measurements. This is expected, since optimizing the model parameters will generally lead to a more sensitive model.

5. **Optimal insulin and glucose release rates.** The feedback controls (2) and (4) model the physiology of the pancreas. Liu and Tang [8] have suggested that these natural feedback controls may not be "optimal" in the sense of regulating the blood glucose level. However, they did not check this conclusively by solving the associated optimal control problem [8]. In this section, we demonstrate that the optimal open loop controls for the insulin and glucose release rates can be readily calculated using the MISER 3.3 software [4]. We replace the closed loop controls w_1 and w_2 by corresponding open loop controls u_1 and u_2, respectively. Thus, equations (1) and (3) become, respectively,

$$\frac{dx_1}{dt} = -(k_{1,1}^p + k_{1,2}^p)x_1 + u_1, \tag{28}$$

and

$$\frac{dx_2}{dt} = -(k_{2,1}^p + k_{2,2}^p)x_2 + u_2. \tag{29}$$

We assume that both u_1 and u_2 are parameterized as piecewise linear continuous functions in accordance with the control parameterization method [7, 12]. The

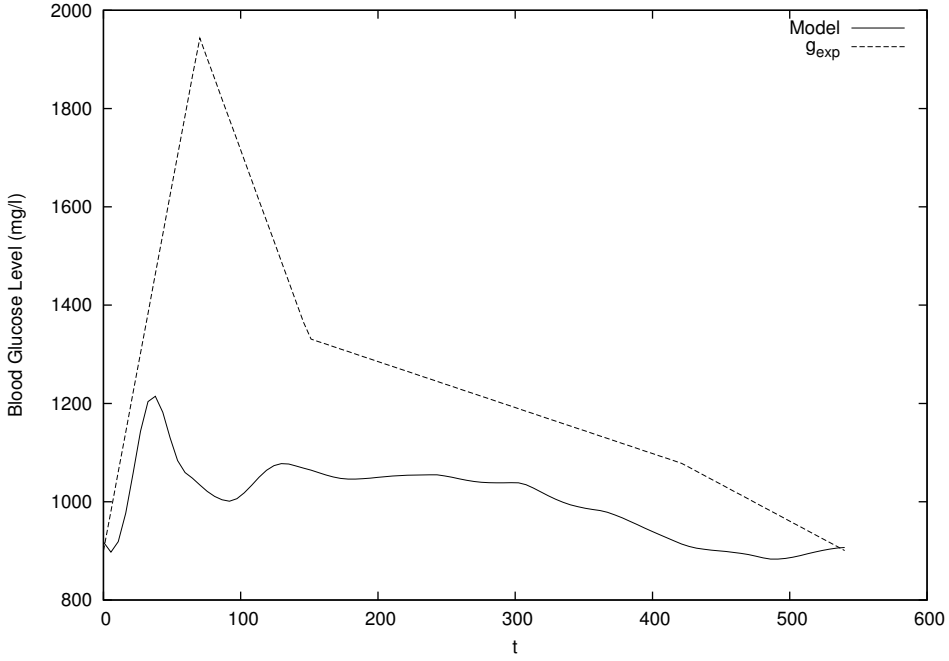

FIGURE 7. Blood glucose level when w_2 is defined by (26).

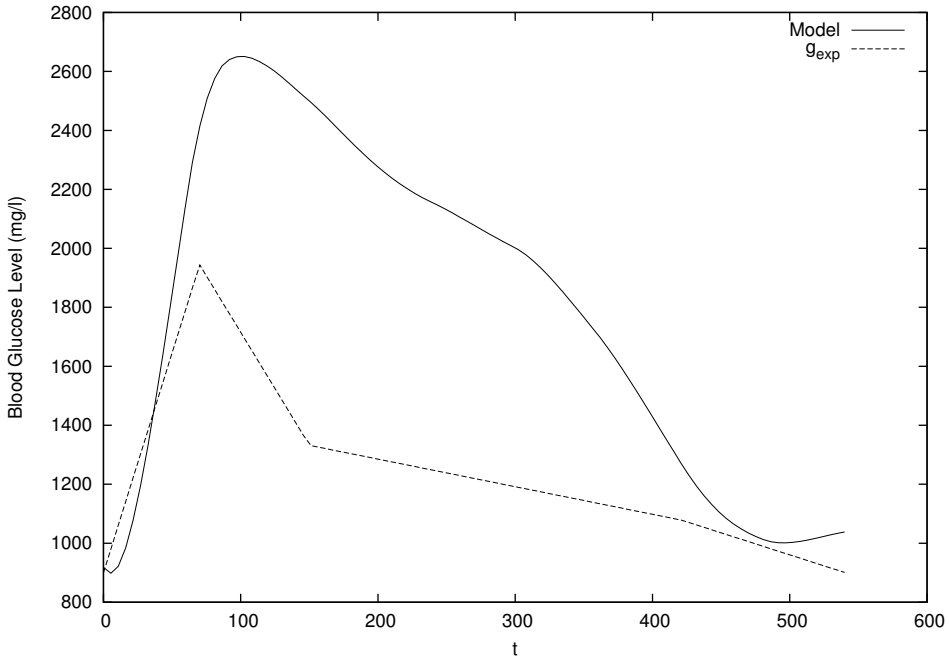

FIGURE 8. Blood glucose level when w_2 is defined by (27).

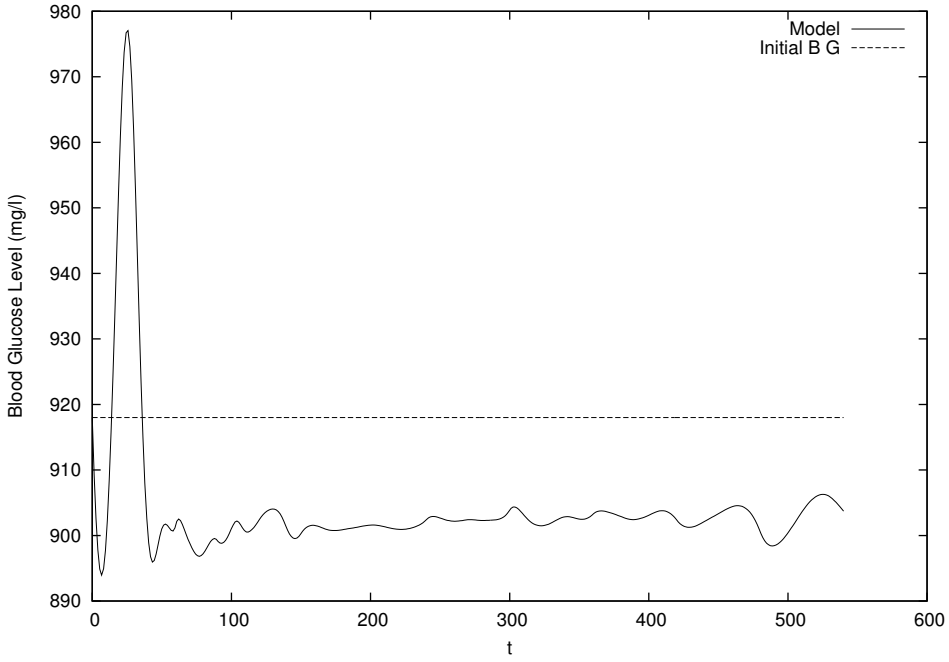

FIGURE 9. Optimal blood glucose trajectory corresponding to the optimal solution in Section 5.

objective function (adopted from the suggestion in [8]) is given by:

$$J = \int_0^{540} \{(x_8(t) - 918)^2 + u_1^2(t) + u_2^2(t)\}dt. \tag{30}$$

This objective function penalizes both control effort and blood glucose deviation from the initial level. The problem is to minimize (30) subject to the dynamic model (1)-(23) with the optimized parameters from Case 1 (and with (1) and (3) replaced by (28) and (29)). As the model is quite sensitive to changes in u_1 and u_2, we use a homotopy approach with the initial guesses of u_1 and u_2 as w_1 and w_2 (from the Case 1 optimized model), respectively. We initially imposed tight lower and upper bounds on u_1 and u_2 around the initial guesses. These bounds were then slowly relaxed over a series of optimization iterations until no more improvement in the objective was observed.

The optimal blood glucose trajectory is shown in Figure 9 and the optimal controls are shown in Figures 10 and 11. As can be seen from Figure 9, the blood glucose level corresponding to the optimal open loop controls remains very close to the initial blood glucose level (918 mg/l= 5.1 mmol/l) over the entire time horizon. This clearly demonstrates that excellent glucose control is achievable with the open loop formulation. However, the blood glucose response is quite different from that observed in experimental results. This raises the question of why the blood glucose regulatory system in the human body does not follow the 'optimal' approach calculated via the open loop formulation. One should note that the glucose regulatory system forms only one part of a more complex metabolic system that controls the human body. There are probably sound reasons why elevated blood glucose levels

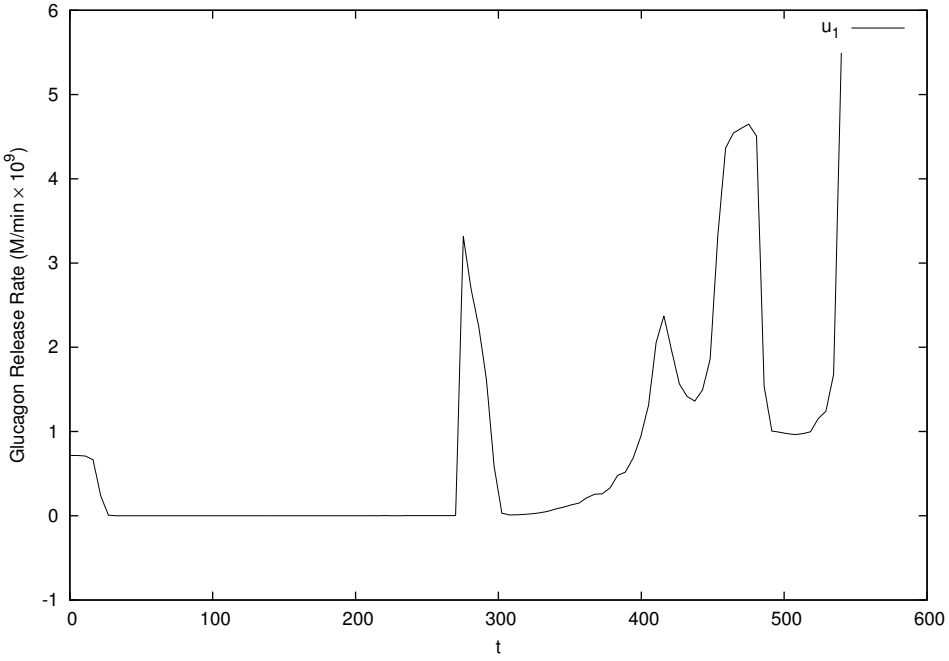

FIGURE 10. The optimal glucagon release rate.

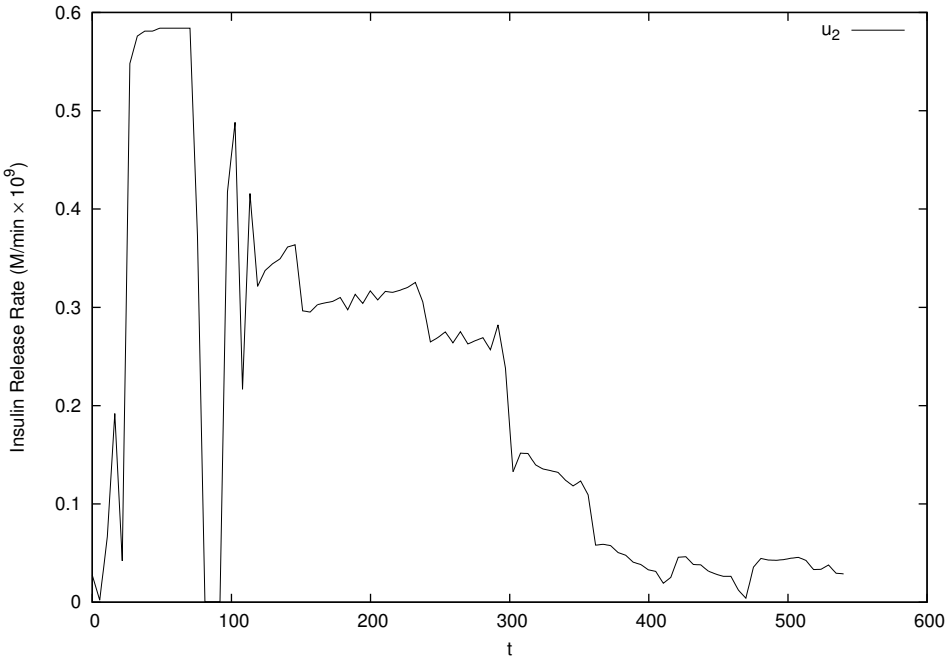

FIGURE 11. The optimal insulin release rate.

occur in humans after the ingestion of a meal, but these are not reflected in the glucose regulatory model considered here.

6. **Conclusions.** We have solved a complex model matching problem in which a glucose regulatory model must be fitted to experimental data to minimize total error. We investigated several different model matching objectives and found that significant improvement in matching the model to experimental data was achieved in all cases when compared to the results in Liu and Tang [8]. As expected, we also found that the optimized model was more sensitive to changes in the insulin release rate. Finally, we showed that open loop optimal controls can be readily calculated for the glucose regulatory system. However, the resulting glucose profiles no longer match real profiles observed experimentally, which suggests that more comprehensive models of the human body metabolism are needed.

Future work will consider the implementation of the glucose regulatory model for diabetic individuals and how their conditions can be controlled optimally.

REFERENCES

[1] F. Chee and T. Fernando, *Closed Loop Control of Blood Glucose*, Springer, Berlin, 2007.
[2] R. Hovorka, V. Canonico, L. J. Chassin, U. Haueter, M. Massi-Benedetti, M. O. Federici, T. R. Pieber, H. C. Schaller, L. Schaupp, T. Vering and M. E. Wilinska, Nonlinear model predictive control of glucose concentration in subjects with type 1 diabetes, *Physiological Measurement,* **25** (2004), 905–920.
[3] IDF Diabetes Atlas, 5th Edition, *International Diabetes Federation*, Brussels, 2011.
[4] L. S. Jennings, M. E. Fisher, K. L. Teo and C. J. Goh, *MISER3 Optimal Control Software: Theory and User Manual Version 3*, University of Western Australia, Perth, 2004.
[5] M. Korach-André, H. Roth, D. Barnoud, M. Péan, F. Péronnent and X. Leverve, Glucose appearance in the peripheral circulation and liver glucose output in men after a large C starch meal, *The American Journal of Clinical Nutrition,* **80** (2004), 881–886.
[6] L. Kovács, B. Kulcsár, A. György and Z. Benyó, Robust servo control of a novel type 1 diabetic model, *Optimal Control Applications and Methods,* **32** (2011), 215–238.
[7] Q. Lin, R. Loxton and K. L. Teo, The control parameterization method for nonlinear optimal control: A survey, *Journal of Industrial and Management Optimization,* **10** (2014), 275–309.
[8] W. Liu and F. Tang, Modelling a simplified regulatory system of blood glucose at molecular levels, *Journal of Theoretical Biology*, **252** (2008), 608–620.
[9] R. Loxton, K. L. Teo and V. Rehbock, Optimal control problems with multiple characteristic time points in the objective and constraints, *Automatica,* **44** (2008), 2923–2929.
[10] G. Marchetti, M. Barolo, L. Jovanovic and H. Zisser, An improved PID switching control strategy for type 1 diabetes, In *Proceeding of the 28th IEEE EMBS Annual International Conference,* New York, (2006), 5041–5044.
[11] R. Martin and K. L. Teo, *Optimal Control of Drug Administration in Cancer Chemotherapy*, World Scientific, Singapore, 1993.
[12] K. L. Teo, C. J. Goh and K. H. Wong, *A Unified Computational Approach to Optimal Control Problems*, Longman Scientific and Technical, Essex, 1991.

Received June 2014; revised September 2014.

E-mail address: alhilalzh@hotmail.com
E-mail address: v.rehbock@curtin.edu.au
E-mail address: r.loxton@curtin.edu.au